Observational Study

Medicine

OPEN

# An integrated bioinformatics analysis identifying ALOX15 as a novel pharmacological target for retinitis pigmentosa and diabetic retinopathy

Weiming Yan, MD[a], Qiurui He, MD[b], Lei Zhang, MD[c,*], Haiyan Wang, MD[a]

**Abstract**

This study aimed to find shared gene signatures, molecular processes, and potential pharmacological targets in retinitis pigmentosa (RP) and diabetic retinopathy (DR) through integrated bioinformatics analysis. Two datasets were downloaded from the Gene Expression Omnibus (GEO) database. Differentially expressed genes were identified using the R software, and co-expression gene weighted expression method (WGCNA) was conducted to find the co-expression networks. Common genes were screened with a Venn tool. Functional and pathway enrichment analyses were performed, and a protein-protein interaction (PPI) network was constructed. Common miRNAs were identified and functionally analyzed. Seven overlapping differentially expressed genes and 2 shared genes from WGCNA core modules were identified. Gene Ontology (GO) analysis highlighted regulation of lipoxin metabolism and membrane-associated oxidoreductase activity. Kyoto Encyclopedia of Genes and Genomes (KEGG) enrichment focused on linoleic and arachidonic acid metabolism, with ALOX15 as the key oxidase. PPI network analysis also emphasized ALOX15. The overlapping miRNA hsa-mir-133b was associated with organelle-related functions. Integrated bioinformatics revealed that the lipoxygenase pathway and membrane oxidoreductase activity likely contribute to RP and DR pathogenesis, with ALOX15 as a promising therapeutic target. ALOX15's role in lipoxin metabolism and oxidative stressed positions it as a novel pharmacological target for preserving retinal function in RP and DR. These findings paved the way for developing targeted therapies to improve visual outcomes in these diseases.

**Abbreviations:** BP = biological processes, CC = cellular components, DEGs = differentially expressed genes, DR = diabetic retinopathy, GEO = Gene Expression Omnibus, GO = Gene Ontology, GS = gene significance, GSE = GEO series, HMDD = human microRNA disease database, iPSCs = induced-pluripotent stem cells, KEGG = Kyoto Encyclopedia of genes and genomes, LXA4 = Lipoxin A4, MCODE = molecular complex detection, ME = module eigengene, MF = molecular functions, MM = module membership, PCA = principal component analysis, PPI = protein-protein interaction network, ROs = retinal organoids, RP = retinitis pigmentosa, RPE = retinal pigment epithelium, STRING = search tool for the retrieval of interacting genes, TOM = topological overlap matrix, TPM = transcripts per million, VEGF = vascular endothelial growth factor, WGCNA = weighted gene co-expression network analysis.

**Keywords:** bioinformatics, diabetic retinopathy, miRNA, retinitis pigmentosa, WGCNA

## 1. Introduction

Retinal degenerative diseases, including retinitis pigmentosa (RP) and diabetic retinopathy (DR), can result in the death of rods and cone photoreceptors, structurally and functionally leading to legal or complete blindness.[1] During RP, an inherited retinal disorder with a prevalence of 1/4000, progressive degeneration of photoreceptor rod cells and retinal pigment epithelium (RPE) is the main characteristic with a clinical sign of bone-like pigmentation.[2] As the disease progresses, the

*This work was supported by grants from the Postdoctoral Science Foundation of the Fuzhou General Hospital (No. 48678), the National Natural Science Foundation of China (No. 82301245), the Joint Funds for the Innovation of Science and Technology, Fujian Province (No. 2024Y9653), the Xi'an Science and Technology Project (No. 24YXYJ0091), the General Cultivation Project of the Municipal Health Commission in Xi'an, China (No. 2024ms18), and the Natural Science Foundation of Fujian Province, China (No. 2024J011148).Prof. Haiyan Wang should be considered as a co-corresponding author as she contributed equally to the conceptualization, research conduction, and revision.*

*Consent for publication was waived because this study used only publicly available data and did not involve human experiments.*

*The authors have no conflicts of interest to disclose.*

*The datasets generated during and/or analyzed during the current study are available from the corresponding author on reasonable request.*

*Ethical approval was waived because this study used only publicly available data and did not involve human experiments.*

*[a] Department of Ophthalmology, Fuzong Clinical Medical College of Fujian Medical University, Dongfang Hospital Affiliated to Xiamen University, Fuzhou, China,*
*[b] Department of Medicine, The Third Hospital of Zhangzhou, Zhangzhou, China,*
*[c] Department of Ophthalmology, Shaanxi Eye Hospital, Xi'an People's Hospital (Xi'an Fourth Hospital), Affiliated Guangren Hospital of Xi'an Jiaotong University, Xi'an, China.*

** Correspondence: Weiming Yan, Fuzong Clinical Medical College of Fujian Medical University, Dongfang Hospital Affiliated to Xiamen University, Fuzhou 350025, China (e-mail: ywming@fjmu.edu.cn).*



*How to cite this article: Yan W, He Q, Zhang L, Wang H. An integrated bioinformatics analysis identifying ALOX15 as a novel pharmacological target for retinitis pigmentosa and diabetic retinopathy. Medicine 2026;105:20(e47569).*

*Received: 29 June 2025 / Received in final form: 11 December 2025 / Accepted: 16 January 2026*

*http://dx.doi.org/10.1097/MD.0000000000047569*

**Table 1**

**Statistics of the 2 data series containing the RP/DR patients derived from GEO database.**

| ID | GSE series | Platform | Samples | Disease | Type of data |
|---|---|---|---|---|---|
| 1 | GSE141531 | GPL24676 | 5 patients and 5 controls | RP | RNA-seq profiles |
| 2 | GSE185011 | GPL24676 | 5 patients and 5 controls | DR | RNA-seq profiles |

DR = diabetic retinopathy, GEO = Gene Expression Omnibus, RP = retinitis pigmentosa.

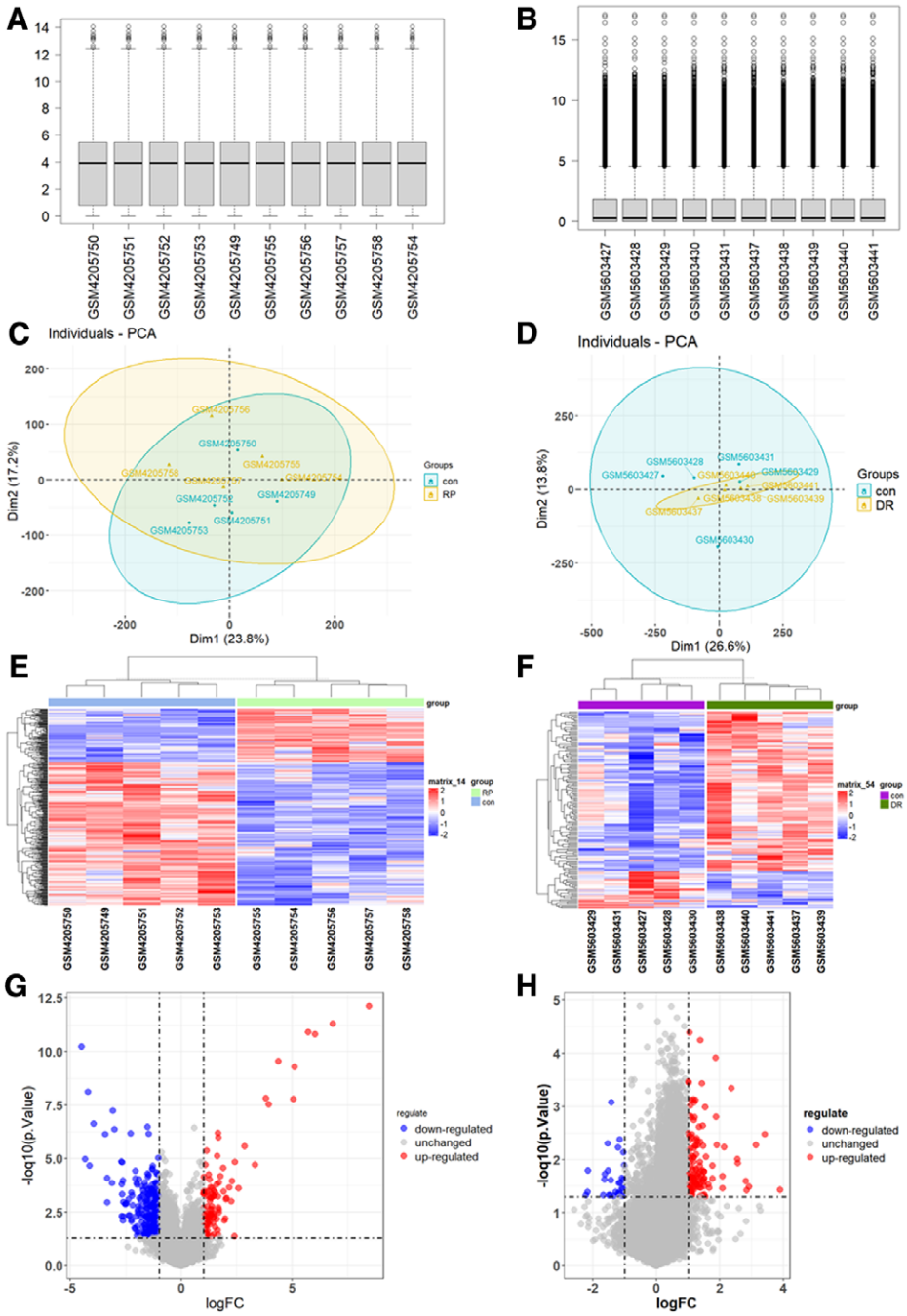


**Figure 1.** The analysis of the DEGs in the RP and DR GSE series. (A, B) The box plot of the distribution of differently expression data series in the analyzed RP and DR GSE data series. (C, D) The cluster plot (PCA plot) of expression data distribution of RP and DR GSE data series. (E, F) The heatmap of the DEGs in RP and DR. Each column represented 1 dataset and each row indicated 1 gene. Blue represented downregulated genes and red represented upregulated genes. (G, H) The volcano plots of the DEGs in RP and DR. The Blue ones represented downregulation, red ones indicated upregulation, and gray ones were the rest of the DEGs. DEGs = differentially expressed genes, DR = diabetic retinopathy, PCA = principal component analysis, RP = retinitis pigmentosa.

cone and retinal vascular systems can also be affected. It develops over the course of several decades; however, the majority of its progression occurs within the first 4 decades after birth. In DR, one of the main ocular complications associated with diabetes, degeneration of the retinal vascular system can gradually lead to damage to retinal function. It affects almost 93

million patients worldwide, with 28 million individuals at risk of becoming blind. Blood levels of glycemia and lipids are considered risk factors for DR.[3] Although RP and DR have been studied for years, their exact mechanisms of interaction remain unknown.[4] Current treatment for PR and DR sometimes cannot significantly improve the quality of life of patients.[5,6] Therefore, the development of therapeutic strategies to preserve retinal function is a favorable asset in the clinic.

The pathogenesis of RP and DR involves a complex interplay of genetic factors that contribute to the onset and progression of these diseases, respectively. Potential genetic pathogenic targets for RP include genes encoding proteins involved in phototransduction, structural components of the retina, and cellular signaling pathways crucial for retinal function.[7] In the case of DR, potential genetic targets may involve genes related to vascular endothelial growth factor (VEGF) signaling, inflammation, oxidative stress, and angiogenesis regulation.[8] Due to the pathological changes involving retinal vasculature pathological change in both RP and DR, whether there are common susceptible pathogenic genes and corresponding mechanisms between the 2 diseases remains an interesting research direction.[9,10] Understanding the potential genetic pathogenic targets is crucial for advancing targeted therapeutic approaches and precision medicine strategies aimed at addressing the underlying causes of RP and DR. However, the possible pathogenic mechanisms and targets shared between RP and DR have not yet been elucidated.

This study aimed to investigate shared gene signatures and molecular processes between RP and DR using data from the Gene Expression Omnibus (GEO). The current methods for identifying potential pathogenic genes through bioinformatics analysis include differential gene analysis and a relatively novel algorithm called co-expression gene weighted expression method (WGCNA). Our research utilized a combination of the 2 methods, with other further multiple bioinformatics analyses for a more robust screening process. Our study finally revealed that the lipoxygenase pathway and oxidoreductase activity in membrane organelles may commonly be involved in the pathogenesis of RP and DR, with ALOX15 identified as a novel possible comon pharmacological target of RP and DR.

## 2. Methods

### 2.1. Data source and Gene expression profile

The GEO database is a public functional genomic repository of high-throughput gene expression data, chips, and microarrays.[11] We used the keywords "retinitis pigmentosa" or "diabetic retinopathy" and "homo sapiens" to search for gene expression profile data of patients with RP and DR in the GEO database (http://www.ncbi.nlm.nih.gov/geo/). The obtained datasets were screened using the following criteria. First, the profile information should include both the case and control groups. Second, these datasets must provide raw data that could be further analyzed. Third, all the samples were derived from human tissues. The GEO Series (GSE) numbered GSE141531 and GSE185011 datasets were finally retrieved for our current study.

In details, the GSE141531 dataset was used for RP analysis. The dataset comprised raw transcriptomic information obtained from retinal organoids (ROs). ROs were derived from induced-pluripotent stem cells (iPSCs) sourced from both RP patients and control subjects. Specifically, the data series comprised 10 specimens, including 5 RP samples and 5 control samples sourced from the original reference.[12] For DR analysis, we utilized the GSE185011 dataset, which contained mRNA and lncRNA expression profiles in peripheral blood from 5 patients with DR and 5 control patients, as reported in the original reference.[13] The gene expression profiles for both datasets were detected using GPL24676 Illumina NovaSeq 6000 (Homo sapiens) for high-throughput sequencing (Table 1).

Original data were acquired and processed via R packages of "GEOqeury" using background correction, normalization, and relative expression calculations. In greater details, quantile normalization (i.e., applied using the normalizeBetweenArrays function from the limma package) was applied on the RNA-seq data in our study to ensure that gene expression levels were comparable across samples. Furthermore, the HTSeqFPKM value was transformed into transcripts per million (TPM), which allows for the comparison of gene expression across both genes and samples. $Log_2$ transformation was applied to gene expression profiling, and the probes were matched with their gene symbols based on annotated files from the relevant platforms. The type of platform used in our study was the RNA-seq. Before analysis, Quantile Normalization was applied to the RNA-seq data used in our study, to make sure that gene expression levels are comparable across samples. Ultimately, we acquired the genetic matrix with rows and columns defined as the specimen names and gene symbols, respectively, for the following analysis. In greater details, the expression levels in both RP and DR series were analyzed via the boxplot. In addition, the data distribution of both series the genes were explored via the Principal Component Analysis (PCA) in R software. Ethical approval was waived because this study used only publicly available data and did not involve human experiments.[14]

### 2.2. Data processing and the differential genes (DEGs) analysis

***2.2.1. Screening of the DEGs.*** The "Limma" package from the R software (Version: *R*-4.5.2 for Windows, 87 megabytes, 64 bit, Released: November, 2025) was applied to analyze the raw data, which was displayed in box plots. $Log_2$ conversion and DEGs screening of matrix data were performed. The adjusted $P$ values $< .05$ were considered statistically significant.[14] Furthermore, genes with $|\log FC \text{ (foldchange)}| >= 1.0$ were chosen for the presence of DEGs samples.[15] Volcano plots and the heatmap were applied to show all upregulated and downregulated DEGs with the R packages of "ggplot2" and "pheatmap." The Venn diagram web tool (http://bioinformatics.psb.ugent.be/webtools/Venn/) was used to identify common DEGs shared between these 2 datasets.

The DEGs of RP or DR satisfying the adjusted $P$-value (<.05) were subjected to WGCNA using the R package, which is a relatively popular bioinformatics algorithm.[16] The WGCNA was used to identify gene co-expression modules with great importance in biology and to discover the relevance between diseases

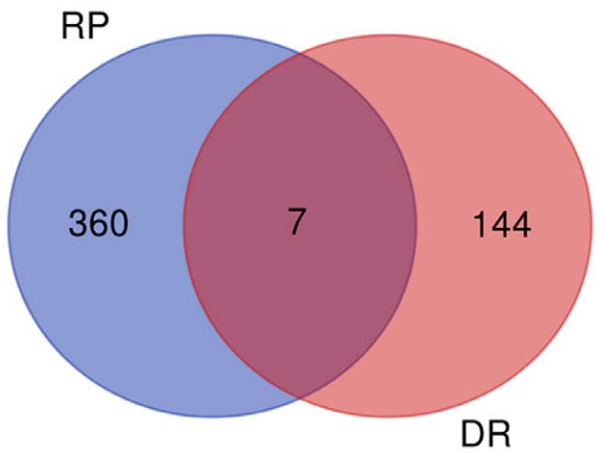


**Figure 2.** The Venn diagram of the common DEGs shared in the RP and DR GSE series. The 2 datasets showed an overlap of 7 genes. DEGs = differentially expressed genes, RP = retinitis pigmentosa, DR = diabetic retinopathy.

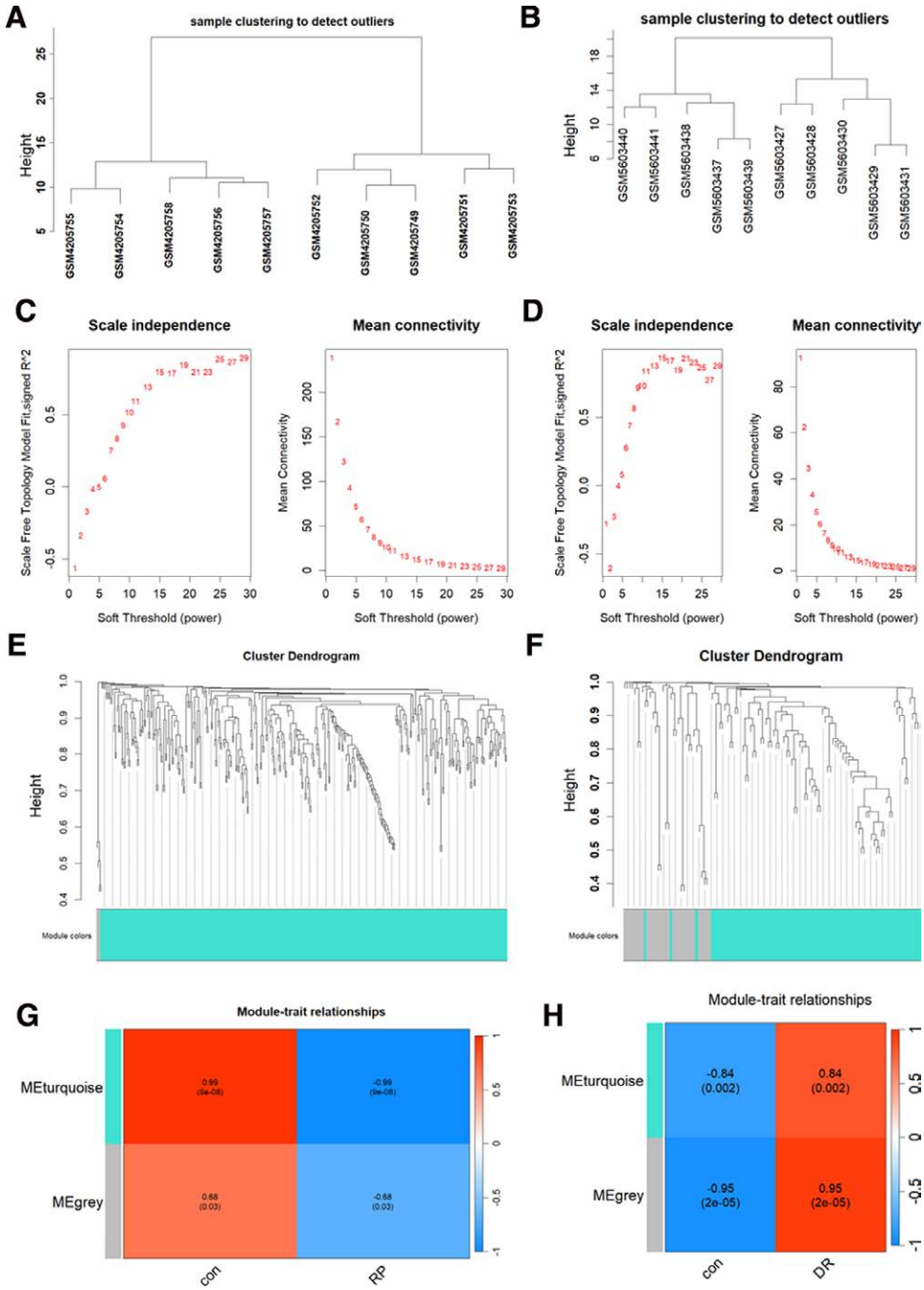


**Figure 3.** The Weighted gene co-expression network analysis (WGCNA) of the DEGs in the RP and DR GSE series. (A, B) The sample clustering of datasets in the analyzed RP and DR GSE data series. (C, D) The Scale independence and mean connectivity of expression data distribution of RP and DR GSE data series. (E, F) The cluster dendrogram of co-expression genes in the analyzed RP and DR GSE data series. (G, H) The Module–trait relationships in RP and DR. Each cell contains the corresponding correlation and *P*-value. The Blue ones represented negative association, red ones indicated positive association. DEGs = differentially expressed genes, DR = diabetic retinopathy, RP = retinitis pigmentosa.

and gene networks.[17] In details, the adjacency matrix was built using a soft threshold by the function of "pickSoftThreshold" in R software, which was aimed for topology calculation and a gene-gene correlation matrix to describe the degree of association between the nodes. According to the optimum soft threshold,[18] the adjacency matrix was converted into a topological overlap matrix (TOM). Next, a gene hierarchical clustering dendrogram was performed to identify co-expression modules. Gene significance (GS) and module membership (MM) in each module were calculated to plot the scatter plots. The module eigengene (ME) was also calculated. Finally, Pearson's correlation analysis was used to estimate the relevance of disease emergence to the merged modules. Modules with high correlation with DR and RP were chosen, and the shared genes in modules related to DR and RP were overlapped using the Venn diagram web tool.

***2.2.2. Gene Ontology (GO) function and Kyoto Encyclopedia of Genes and Genomes (KEGG) pathway enrichment analyses of DEGs.*** To analyze the function of the common DEGs or the shared identified genes, the GO function was conducted using the above R software with the "Bioconductor" and "GOplot" packages.[19] The analysis was divided into 3 categories: biological processes (BP), cellular components (CC), and molecular functions (MF). In addition, KEGG pathway

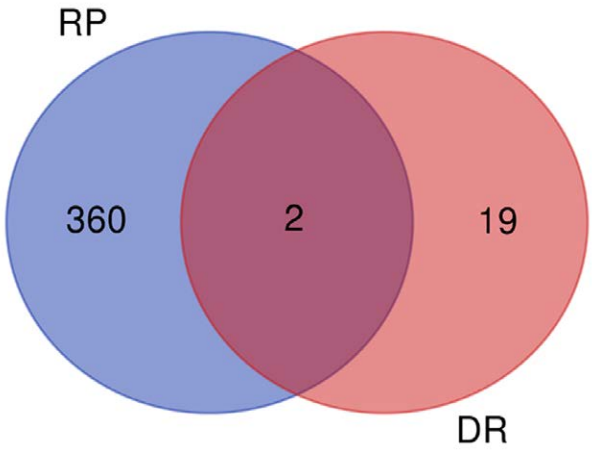


**Figure 4.** The Venn diagram of the common shared genes in the relevant core modules of RP and DR GSE series. Two genes were crossed and overlapped in the relevant core modules of RP and DR. RP = retinitis pigmentosa, DR = diabetic retinopathy.

enrichment analysis was conducted under the R software function of "enrichKEGG," to understand high-level functions and biological systems from large-scale molecular datasets generated using high-throughput experimental technologies. The cutoff criterion for GO and KEGG was an adjusted *P*-value < .05.[20,21] Finally, the plots for GO and KEGG results were conducted under the functions of "barplot" and "dotplot" in the R software, with the KEGG images sourced from the pathway database copyrighted by Kanehisa laboratories.[22]

***2.2.3. Protein-protein interaction network (PPI) construction and module analysis.*** The Search Tool for the Retrieval of Interacting Genes (STRING; http://string-db.org/) (version 11.0) online database was used to predict the network among common DEGs or shared identified genes of RP and DR. In greater details, the confidence score was set at > 0.7, and the species was limited to H. sapiens in the STRING analysis.[23] Furthermore, the PPI networks were constructed using Cytoscape software (http://www.cytoscape.org/, version 3.8.0).[24] Subsequently, key modules from the PPI network were identified using the Cytoscape plug-in for molecular complex detection (MCODE). All interacting data were entered into the Cytoscape software for visualization.

***2.2.4. Prediction of common miRNA and the functional enrichment analysis.*** The Human microRNAs Disease Database (HMDD, http://www.cuilab.cn/hmdd)[25] was used to search for miRNAs related to both RP and DR. The Venn diagram tool was further applied to identify the common miRNAs shared between DR and RP. In addition, functional enrichment analysis, including GO and KEGG analyses, of common miRNAs was performed via the online software of DIANA-miRPath v3.0 (http://www.microrna.gr/miRPathv3).[26] The heatmap format was then shown according to the miRTarbase, miRDB, and TargetScan databases.

## 3. Results

### *3.1. Identification of common DEGs across 2 GSEs between RP and DR*

In the 2 data series selected from the GEO database, the expression levels in each series were almost the same as shown in the boxplot (Fig. 1A, B). In addition, the genes were well clustered between the RP and control groups and were also well clustered between the DR and control groups shown in the PCA plot (Fig. 1C, D). In total, 367 and 151 DEGs were obtained from the RP and DR data series, respectively. The expression levels of all the DEGs were presented in the heatmap, where blue grids represented the downregulation and red grids indicated upregulation of DEGs (Fig. 1E, F). In addition, all DEGs were plotted in volcano plots, in which blue ones represented downregulation, red ones indicated upregulation, and gray ones represented the rest of the DEGs (Fig. 1G, H). There were 207 downregulated DEGs and 160 upregulated ones between RP and matched healthy samples. Meanwhile, 27 downregulated DEGs and 124 upregulated ones were identified between DR samples and matched healthy samples. Furthermore, overlap of the DEGs of RP and DR revealed 7 common DEGs: MEST, CDNK1C PLD4, SYNPO, PAX5, LPAR6, and ALOX15, as shown in the Venn diagram (Fig. 2), containing 3 upregulated genes and 4 downregulated ones.

### *3.2. The co-expression modules and the gene signatures in RP and DR*

The 2 disease samples of DR and RP clustered well according to the clustering trees in WGCNA analysis (Fig. 3A, B). To obtain an appropriate mean connectivity, we applied soft thresholds ranging from 1 to 30, resulting in thresholds of 21 and 13 for the RP and DR datasets, respectively. The gene modules were then cut to a height of 0.7[27] (Fig. 3C, D).

Specifically, we identified 2 distinctly significant modules with different colors, "turquoise" and "gray," in RP data series of GSE141531. For the correlation analysis, RP was encoded as the trait variable. In details, RP was encoded as a binary variable, with "1" representing RP patients and "0" representing healthy controls. A heatmap using the Spearman's correlation coefficients to investigate their relevance to RP was further created under WGCNA. The results revealed that both the "turquoise" and "gray" modules were highly negatively associated with RP, indicating that they could be considered RP-related modules (turquoise module: r = –0.99, *P* = 9e – 08; gray module: r = –0.68, *P* = .03). The negative Spearman correlation implied that lower expression levels of genes within the module were associated with the presence of RP, implying a potential downregulation of these gene networks in RP patients. Notably, the " turquoise " module had the highest relevance to RP, as the *P*-value was smaller than that of the other module. (Fig. 3E, G).

Additionally, we identified 2 modules in total by WGCNA in GSE185011 to assess the relationship between DR and gene expression profiles. The heatmap on the basis of Spearman correlation coefficient showed that the "turquoise" module (*R* = 0.84, *P* = .029e – 04) and "gray" (*R* = 0.95, *P* = 2e – 05), were highly positively linked with DR. Among them, the "gray" module showed the strongest positive association with DR (Fig. 3F, H).

In the RP dataset, all genes within the "turquoise" module were extracted, comprising a total of 362 genes. Similarly, in the DR dataset, all genes within the "gray" module were extracted, with a total of 21 genes. Furthermore, 2 common genes, MEST and ALOX15, were crossed and overlapped in the relevant core modules of both RP and DR shown in the Venn diagram (Fig. 4).

### *3.3. The GO and KEGG enrichment analysis of the common DEGs and the shared genes in the relevant core modules of RP and DR*

To obtain deeper insight into the biological functions of the common DEGs and shared genes in the relevant core modules of RP and DR, GO annotation and KEGG pathway enrichment analyses were performed.

GO analysis showed that the BP terms of the common DEGs focused mainly on the regulation of supramolecular fiber organization, lipoxin metabolic process, positive regulation of cytoskeleton organization, hepoxilin metabolic process,

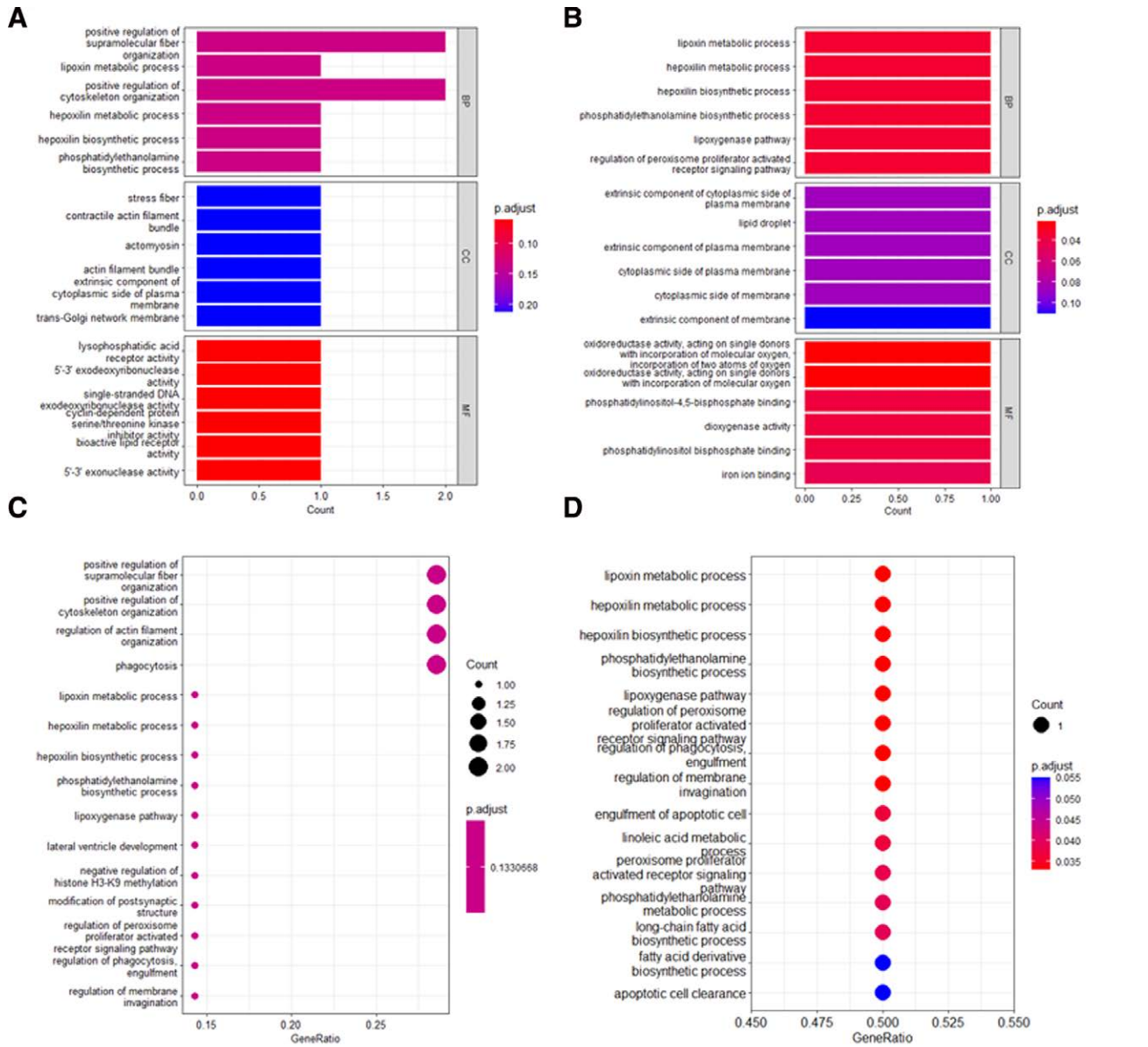


**Figure 5.** GO analysis of the common DEGs and the shared genes in the relevant core modules between RP and DR. (A, C) The GO analysis of the common DEGs between DR and RP. (B, D) The GO analysis of the shared genes in the relevant core modules between DR and RP. Each cell contains the corresponding GO analysis and *P*-value. BP = biological process, CC = cellular component, DEGs = differentially expressed genes, DR = diabetic retinopathy, GO = gene ontology analysis, MF = molecular function, RP = retinitis pigmentosa.

and hepoxilin biosynthetic process. The main related gene was ALOX15. However, the *P* values were >.05 (all *P* = .133). (Fig. 5A, C)

The BP terms of shared genes in the relevant core modules of RP and DR were mainly enriched in the lipoxin metabolic process, hepoxilin metabolic process (*P* = .033), hepoxilin biosynthetic process (*P* = .033), phosphatidylethanolamine biosynthetic process, lipoxygenase pathway (*P* = .033), regulation of peroxisome proliferator activated receptor signaling pathway (*P* = .033), regulation of phagocytosis (*P* = .033), engulfment, regulation of membrane invagination (*P* = .033), engulfment of apoptotic cells (*P* = .037), and linoleic acid metabolic process (*P* = .037). The related gene was ALOX15, with *P* values <.05 (Fig. 5B, D)

CC terms of the common DEGs were markedly enriched in stress fibers (*P* = .024), contractile actin filament bundles (*P* = .024), actomyosin actin filament bundles (*P* = .027), and extrinsic components of the cytoplasmic side of the plasma membrane (*P* = .034). The main related genes were SYNPO and ALOX15, with *P* values <.05. (Fig. 5A, C)

Meanwhile, the CC analysis of the shared genes in the relevant core modules of RP and DR were mainly enriched in the cytoplasmic side of the plasma membrane, lipid droplets, extrinsic component of the plasma membrane, cytoplasmic side of the plasma membrane, and cytoplasmic side of the membrane. The related gene was ALOX15. However, the *P* values were more than 0.05 (all *P* = .086). (Fig. 5B, D)

For MF analysis of the common DEGs, the most significantly enriched terms were lysophosphatidic acid receptor activity, 5'-3' exodeoxyribonuclease activity, single-stranded DNA exodeoxyribonuclease activity, cyclin-dependent protein serine/threonine kinase inhibitor activity, and bioactive lipid receptor activity. The main related genes were LPAR6, PLD4, CDKN1C, and LPAR6. However, the *P* values were more than 0.05 (all *P* = .061). (Fig. 5A, C)

The MF terms of shared genes in the relevant core modules focused mainly on oxidoreductase activity (*P* = .011), acting on single donors with the incorporation of molecular oxygen (*P* = .011), incorporation of 2 oxygen atoms (*P* = .020),

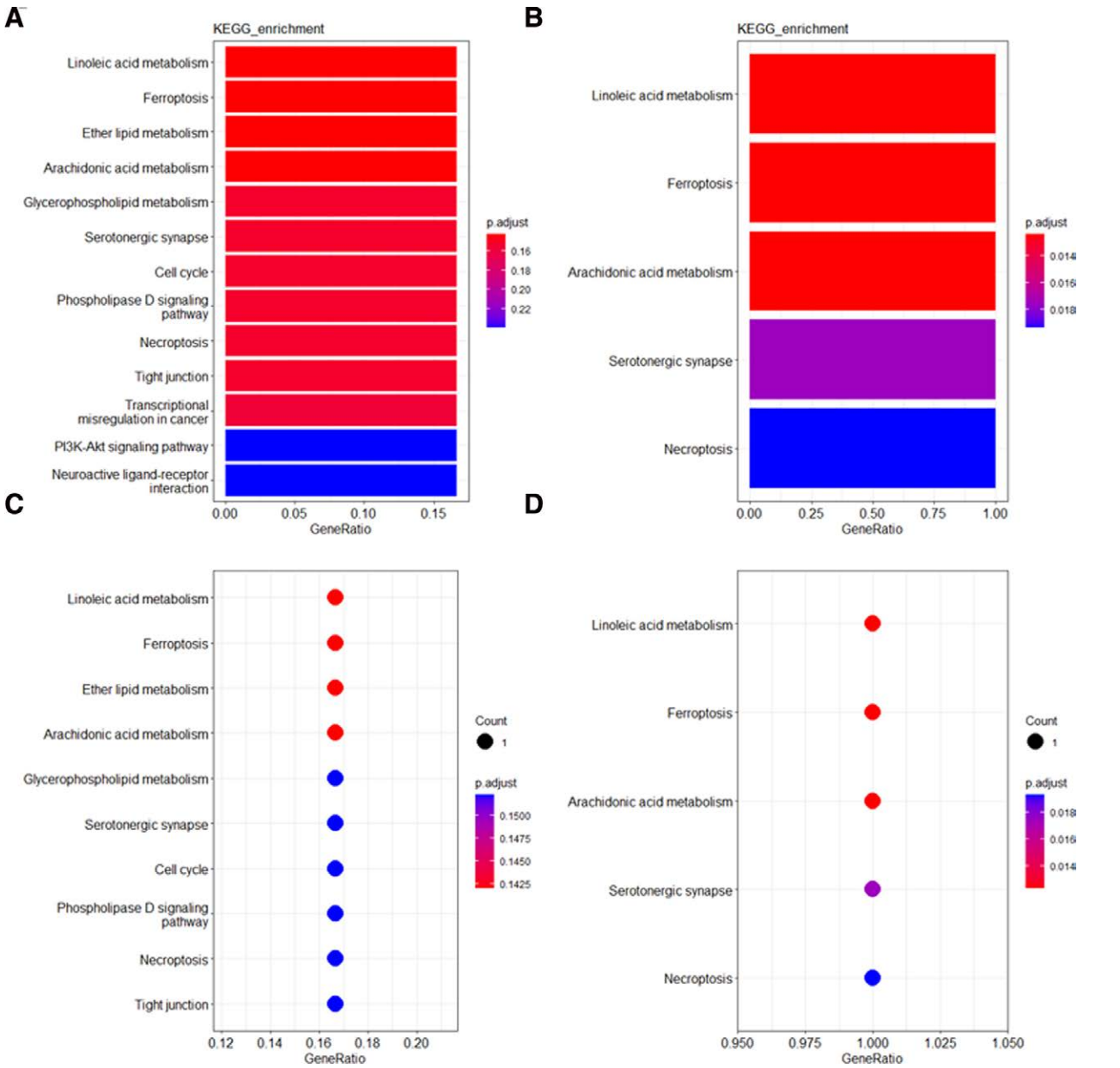


**Figure 6.** KEGG pathway enrichment analysis[22] of the common DEGs and the shared genes in the relevant core modules between RP and DR. (A, C) KEGG pathway enrichment analysis of the common DEGs between RP and DR. (B, D) KEGG pathway enrichment analysis of the shared genes in the relevant core modules between RP and DR. Each cell contains the corresponding KEGG analysis and *P*-value. DEGs = differentially expressed genes, DR = diabetic retinopathy, KEGG = kyoto encyclopedia of genes and genomes, RP = retinitis pigmentosa.

oxidoreductase activity ($P = .020$), acting on single donors with the incorporation of molecular oxygen ($P = .020$), phosphatidylinositol-4,5-bisphosphate binding, dioxygenase activity ($P = .023$), phosphatidylinositol bisphosphate binding, iron ion binding ($P = .023$), phosphatidylinositol phosphate binding ($P = .031$), phosphatidylinositol binding, and phospholipid binding ($P = .048$). The related gene was ALOX15, with *P* values <.05. (Fig. 5B, D)

KEGG analysis revealed that the enriched pathways of common DEGs were linoleic acid metabolism ($P = .142$), ferroptosis ($P = .142$), ether lipid metabolism ($P = .142$), arachidonic acid metabolism ($P = .142$), and glycerophospholipid metabolism ($P = .152$). The related genes were ALOX15 and PLD4. However, the *P* values were >.05. (Fig. 6A, C). Meanwhile, KEGG pathway analysis of the shared genes in the relevant core modules of RP and DR were mainly enriched in linoleic acid metabolism ($P = .012$), ferroptosis ($P = .012$), arachidonic acid metabolism ($P = .012$), serotonergic synapse ($P = .017$), and necroptosis ($P = .019$). The related gene was ALOX15, with *P* values <.05. (Fig. 6B, D).

The GO and KEGG analysis of the DEGs and shared genes in the relevant core modules of RP and DR together showed that the common biological functions focused on lipoxin metabolic process, lipoxygenase pathway, and oxidoreductase activity, of which the common related gene was ALOX15.

### *3.4. PPI network construction and module analysis of the common DEGs and the shared genes in the relevant core modules of RP and DR*

The PPI network of common DEGs and shared genes in the relevant core modules of RP and DR was predicted using STRING. Seven nodes (genes) and 2 edges (interactions) were established in the constructed PPI network of the common DEGs in RP and DR. Interaction between MEST and CDNK1C was found,

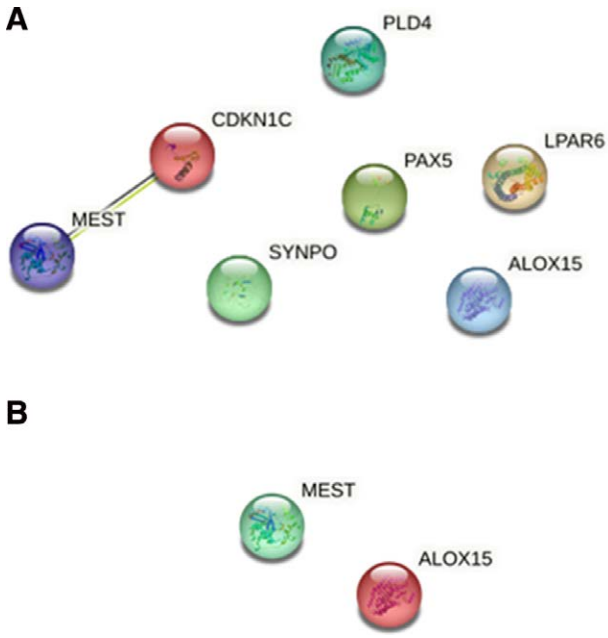


**Figure 7.** The PPI network of the common DEGs and the shared genes in the relevant core modules of RP and DR. (A) PPI network of the common DEGs in RP and DR genes. (B) PPI network of the shared genes in the relevant core modules of RP and DR. The names and abbreviations of the genes were shown besides the nodes. DEGs = differentially expressed genes, DR = diabetic retinopathy, PPI = protein-protein interaction, RP = retinitis pigmentosa.

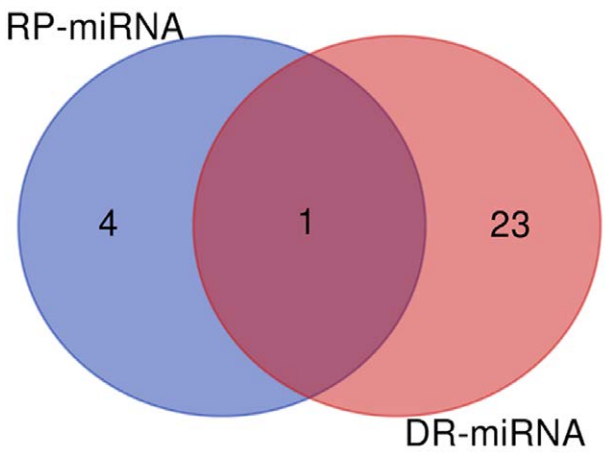


**Figure 8.** The Venn diagram of the common miRNAs of RP and DR. One miRNA was crossed and overlapped in of RP and DR according to the Human microRNA Disease Database (HMDD). RP = retinitis pigmentosa, DR = diabetic retinopathy.

whereas no interactions existed among the other 5 genes (PLD4, SYNPO, PAX5, LPAR6, and ALOX15) (Fig. 7A). Meanwhile, the PPI network of the shared genes in the relevant core modules of RP and DR showed that 2 nodes with zero edges were presented in RP and DR (Fig. 7B). The 2 genes, MEST and ALOX15, did not interact with each other.

### *3.5. Prediction of common miRNAs and the enrichment analysis in RP and DR*

According to the HMDD, 5 miRNAs were found to be related to RP and 24 miRNAs were related to DR. There was 1 overlapping miRNA (hsa-mir-133b) between RP and DR, as shown by the Venn diagram (Fig. 8).

Enrichment analysis of the overlapping miRNA was performed using the miRTarbase, miRDB, and TargetScan databases. A variety of the biological functions of the common miRNA were shown to be involved with the organelles, cellular nitrogen compound metabolic processes, ion binding, RNA binding, biosynthetic processes, cellular components, cellular protein modification processes, poly(A) RNA binding, protein complexes, and nucleic acid binding transcription factor activity (all $P < .01$). Specially, the main common overlapping biological function from the 3 databases of miRTarbase, miRDB, and TargetScan databases was the organelle according to the heatmap (Fig. 9). The organelle was in accordance with the CC analysis from GO, which mainly located in the plasma membrane.

## 4. Discussion

RP and DR are 2 common retinal degenerative diseases that are associated with dysfunction of the retinal vascular system. Despite recent advances in pharmacotherapy and revascularization strategies, RP and DR continue to be the leading threats to visual health worldwide. Therefore, identifying effective treatments that could decrease these harmful effects is of utmost importance.[28] In our study, we conducted an integrated bioinformatics analysis to identify common key genes and molecular processes potentially involved in RP and DR. In details, 2 mRNA microarray datasets of RP tissues and DR tissues were firstly analyzed by "Limma" package from the R software to obtain the DEGs, which containing 160 upregulated genes and 207 downregulated genes in RP, and 124 upregulated genes and 27 downregulated ones in DR. With the help of Venn diagram, there were 7 common DEGs between RP and DR, which were CDKN1C, ALOX15, PLD4, MEST, SYNPO, PAX5, and LPAR6. WGCNA is based on a previously described algorithm for identifying significant gene modules,[29] which was then utilized for the acquisition of gene modules bound to DR and RP in our study. WGCNA constructs a topological matrix of gene expression data and utilizes the properties of a scale-free network to rank genes. By calculating the correlation between genes, it identifies highly co-expressed gene modules. These modules are then correlated with clinical traits (such as disease states), allowing the identification of gene modules and their associated genes that are closely linked to the disease traits. Through the co-expression networks of the WGCNA analysis, we found that the "turquoise" module in the RP dataset was highly correlated with the RP traits, while the "gray" module in the DR dataset was strongly associated with the DR traits. Consequently, we further inferred that the gene expressions within these 2 modules were respectively highly correlated with the RP and DR traits. Drawing support from WGCNA, we identified 2 shared DEGs in the relevant core modules of RP and DR, MEST, and ALOX15. Our results indicated that these selected common genes may be related to the common mechanisms of RP and DR.

To obtain a deeper insight into the biological functions of the selected common genes, the GO and KEGG pathway enrichment analyses were performed.[30] Our results found out that the BP was mainly enriched in the regulation of lipoxin metabolic process, lipoxygenase pathway, peroxisome proliferator activated receptor signaling pathway, and regulation of apoptotic cells. The CC was mainly located in the plasma membrane and includes lipid droplets. MF mainly focused on regulation of oxidoreductase activity. The KEGG pathway of KEGG mainly enriched in linoleic acid and arachidonic acid metabolism, which were also related to oxidoreductase activity and the lipoxygenase pathway in the plasma membrane.[31] Thus, our analysis revealed that the common biological functions of the selected genes of RP and DR lied in the lipoxygenase signaling pathway.

As is known, the lipoxygenase signaling pathway regulates the expression of various genes, including those involved in fatty acid degradation.[32] Highly enriched polyunsaturated fatty acids,

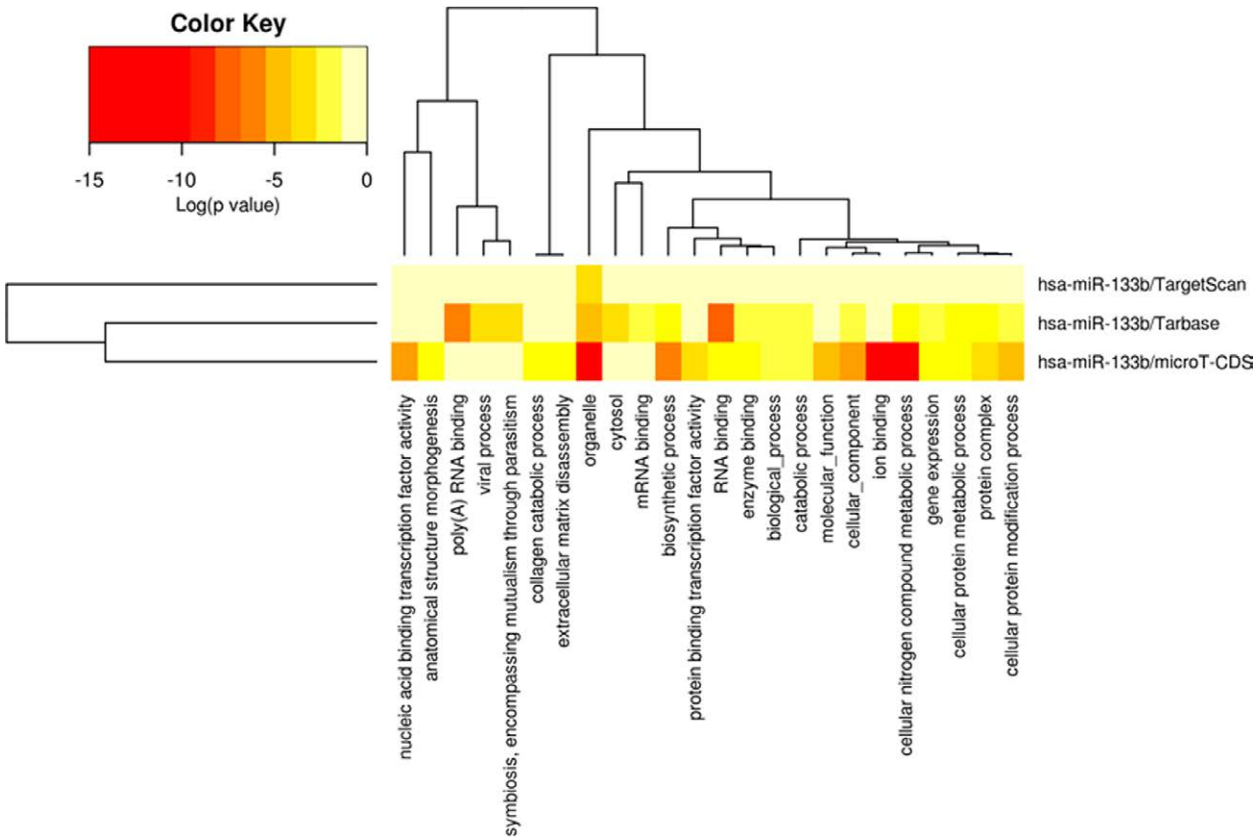


**Figure 9.** The enrichment analysis of common miRNA in RP and DR. The main common overlapped biological function from the 3 databases included the organelle according to the heatmap from the miRTarbase, miRDB, and Targetscan databases. RP = retinitis pigmentosa, DR = diabetic retinopathy.

such as arachidonic acid, in the retina are precursors to oxidized metabolites, namely lipoxin, which can exert pro-inflammatory or antiinflammatory effects under different pathological conditions.[33] Lipoxin in the plasma membrane can be regarded as a bioactive metabolite produced by lipooxygenase enzymes that metabolize arachidonic acid. Therefore, regulation of oxidoreductase activity is vital to the lipoxygenase pathway, which might be related to both RP and DR.[34,35] Zhao et al evaluated the differences of lipoxin levels in the vitreous obtained from 41 patients with DR and 22 non-DR control subjects. Their finding confirmed that elevated levels of some oxylipinsappeared to be associated with imbalanced inflammation-resolution processes in DR and implicated an underlying homeostasis.[36] Lin et al compared the levels of proangiogenic arachidonic acid-derived mediators in human vitreous humor obtained from eyes with high-risk DR vs controls. Their results indicated that lipoxygenase was elevated in the vitreous humor of eyes with high-risk DR, which provided further insight into the pathogenesis of DR and the development of potential therapeutic agents that target arachidonic acid metabolites to treat DR.[37] Besides, a 2-year study on the redox status and visual function of RP patients conducted by Olivares-Gonzalez L et al found that the levels of oxidative stress and lipid peroxidation were elevated in RP and that long-term nutraceutical supplementation could slow down visual impairment in RP.[38] Studies of animal models also demonstrated that modulation of lipoxygenase activity played a significant role in retinal diseases. For example, inhibition of 5-Lipoxygenase in a mouse model of sodium iodate-induced retinal degeneration reduced oxidative stress, lipid peroxidation, and retinal cell death, highlighting the potential of targeting the lipoxygenase pathway in retinal diseases.[39] Similarly, in an oxygen-induced ischemic retinopathy model, inhibition of 12-lipoxygenase significantly reduced retinal neovascularization, offering further evidence that lipoxygenase enzymes may serve as crucial therapeutic targets in retinal pathologies such as DR and RP.[40] The results of the above studies were somewhat in accordance with ours, indicating that the lipoxygenase pathway and oxidoreductase activity in the plasma membrane might be implicated in the pathogenesis of RP and DR.

Furthermore, the main common gene related to the above the GO and KEGG pathway of RP and DR from our enrichment analysis was found to be ALOX15. In greater detail, our PPI network analysis of the selected common genes did not reveal any interaction between ALOX15 and other genes under the application of STRING and Cytoscape, as by other studies.[41] ALOX15, a 5-lipoxygenase, is an oxidizing enzyme that produces reactive lipid hydroperoxide and could biosynthesize Lipoxin A4 (LXA4), which is the first lipid mediator to display antiinflammatory and pro-resolving activities. Elmasry et al found that ALOX15 mediated the inflammatory reaction in the in vivo and in vitro models of DR, in which ALOX15 also regulated the perturbation of calcium homeostasis endoplasmic reticulum stress, and microvascular dysfunction.[42] Viita et al explored the effects of ALOX15 on the VEGF-A(165)-induced retinal angiogenesis, a vital sign of DR, in New Zealand White rabbits' eyes and found that ALOX15 prevented angiogenesis and the consequent pathology.[43] Lu et al assessed the expression of ALOX15 in a mouse model of RP and found a significant upregulation at PN14 and a substantial decrease in the late stage, which might be a compensatory manner during the RP progression.[44] Recently, Ahluwalia K et al revealed a notable decrease in AlOX15 expression in the Royal College of Surgeons (RCS) rat, a well-established disease model for RP. Their studies suggested a possible reduction in antiinflammatory and pro-resolving lipid mediators with the low-expression of ALOX15 in retinal degenerative diseases.[45] The above preliminary studies

were in accordance with our bioinformatics analysis to some extent, which suggest that ALOX15 might be a novel potential treatment target for RP and DR.

MiRNAs, as endogenous noncoding regulatory RNA, play significant roles in the regulation of posttranscriptional genes.[46] In our study, we attempted to identify the common miRNAs in RP and DR using the HMDD, miRTarbase, miRDB, and Targetscan databases.[27] Among these miRNAs, hsa-mir-133b was the common overlapped one between RP and DR. In greater details, our analysis revealed that the biological function of the common miRNA from the 3 databases included organelles, according to the heatmap. This signified that common miRNAs associated with the pathogenesis of RP and DR could also regulate organelles, which were related to the plasma membrane, lipid droplets, and extrinsic components of the plasma membrane.[47,48] The above result was in accordance with our GO and KEGG pathway enrichment analysis of common genes in RP and DR.

Our study has some limitations. Firstly, the sample size of the microarray dataset used in our study was relatively small. Secondly, although we identified enriched pathways and core genes, the hierarchical processes between them were not fully elucidated. Thirdly, the number of common DEGs for RP and DR identified in our study was relatively small, of which the evaluation of ontology and even signaling pathways might not show a very high accuracy. Besides, we relied on the public datasets and bioinformatics analysis to get the results, which required additional research to validate and extend the findings. For example, we would verify the involvement of the ALOX15 gene and related pathways in RP and DR models through carrying out animal or cell experiments. In details, we would investigate the effects of regulating the expression of the gene on the progression of RP and DR by means of gene or protein expression interventions. If possible, we need to collect relevant clinical samples from RP and DR patients to validate our results. In addition, further studies with larger sample sizes with more genes for evaluation are warranted to identify potential biomarkers associated with RP and DR.

## 5. Conclusions

In conclusion, using bioinformatics analysis, our present study identified core common genes between RP and DR, which revealed that the lipoxygenase pathway and oxidoreductase activity in the membrane organelle might be the common pathogenesis of RP and DR. In particular, ALOX15, which could regulate the above biological processes, might be a potential biomarker and therapeutic target for RP and DR. The novel contribution of our current study lied in the comprehensive application of bioinformatics analysis to identify and define common pathogenic cellular pathways and gene targets for RP and DR, based on high-throughputdata from human samples. Further studies of regulating the ALOX5 expression level on animal or cell experiments are needed to elucidate the biological function and underlying mechanisms.

## Acknowledgements

We would like to thank Prof Yubin Liu from the Fujian Normal University for their valuable feedback and discussions. We are also grateful to our families for their constant support and encouragement throughout this study.

## Author contributions

**Conceptualization:** Lei Zhang, Weiming Yan, Qiurui He, Haiyan Wang.
**Data analysis:** Qiurui He.
**Data curation:** Lei Zhang, Qiurui He, Weiming Yan, Haiyan Wang.
**Writing – original draft:** Lei Zhang, Weiming Yan, Haiyan Wang.
**Writing – review & editing:** Lei Zhang, Weiming Yan, Haiyan Wang.
**Formal analysis:** Qiurui He, Weiming Yan, Haiyan Wang.
**Investigation:** Qiurui He, Weiming Yan, Haiyan Wang.
**Methodology:** Weiming Yan, Qiurui He.
**Funding acquisition:** Weiming Yan, Haiyan Wang.
**Project administration:** Weiming Yan, Haiyan Wang.

## References

[1] Kaur G, Singh NK. Inflammation and retinal degenerative diseases. Neural Regen Res. 2023;18:513–8.
[2] Ngo WK, Jenny LA, Kim AH, Kolesnikova M, Greenstein VC, Tsang SH. Correlations of full-field stimulus threshold with functional and anatomical outcome measurements in advanced retinitis pigmentosa. Am J Ophthalmol. 2023;245:155–63.
[3] Yau JWY, Rogers SL, Kawasaki R, et al. Global prevalence and major risk factors of diabetic retinopathy. Diabetes Care. 2012;35:556–64.
[4] Massengill MT, Ahmed CM, Lewin AS, Ildefonso CJ. Neuroinflammation in retinitis pigmentosa, diabetic retinopathy, and age-related macular degeneration: a minireview. Adv Exp Med Biol. 2018;1074:185–91.
[5] Perais J, Agarwal R, Evans JR, et al. Prognostic factors for the development and progression of proliferative diabetic retinopathy in people with diabetic retinopathy. Cochrane Database Syst Rev. 2023;2:CD013775.
[6] Xue Y, Sun X, Wang SK, Collin GB, Kefalov VJ, Cepko CL. Chromophore supply modulates cone function and survival in retinitis pigmentosa mouse models. P Natl Acad Sci USA. 2023;120:e2077082176.
[7] Baz-Redon N, Sanchez-Bellver L, Fernandez-Cancio M, et al. Primary ciliary dyskinesia and retinitis pigmentosa: novel RPGR variant and possible modifier gene. Cells Basel. 2024;13:524.
[8] Alidoust L, Sharafshah A, Keshavarz P. Haplotype-based association study of TCF7L2 gene variants with the development of diabetic retinopathy in an Iranian population. Ophthalmic Genet. 2024;45:226–32.
[9] Yan WM, Long P, Chen MZ, et al. Retinal neovascularization induced by mutant Vldlr gene inhibited in an inherited retinitis pigmentosa mouse model: an in-vivo study. Int J Ophthalmol. 2021;14:990–7.
[10] Kawaguchi Y, Takahashi A, Nagaoka T, Ishibazawa A, Ishiko S, Yoshida A. Retinal and choroidal hyperreflective foci on spectral-domain optical coherence tomographic images in a patient with retinitis pigmentosa accompanied by diabetic retinopathy. Am J Ophthalmol Case Rep. 2016;3:25–30.
[11] Chicco D. geneExpressionFromGEO: an r package to facilitate data reading from Gene Expression Omnibus (GEO). Methods Mol Biol. 2022;2401:187–94.
[12] Gao ML, Lei XL, Han F, et al. Patient-specific retinal organoids recapitulate disease features of late-onset retinitis pigmentosa. Front Cell Dev Biol. 2020;8:128.
[13] Hui Z, Chen YM, Gong WK, et al. Shared and specific biological signalling pathways for diabetic retinopathy, peripheral neuropathy and nephropathy by high-throughput sequencing analysis. Diabetes Vasc Dis Res. 2022;19:14791641221122918.
[14] Kang X, Bai L, Qi X, Wang J. Screening and identification of key genes between liver hepatocellular carcinoma (LIHC) and cholangiocarcinoma (CHOL) by bioinformatic analysis. Medicine (Baltimore). 2020;99:e23563.
[15] Bober P, Tkacikova S, Talian I, Urdzik P, Toporcerova S, Sabo J. Differential urinary proteomic analysis of high-risk cervical intraepithelial neoplasia. Int J Mol Sci. 2023;24:2531.
[16] Rezaei Z, Ranjbaran J, Safarpour H, et al. Identification of early diagnostic biomarkers via WGCNA in gastric cancer. Biomed Pharmacother. 2022;145:112477.
[17] Langfelder P, Horvath S. WGCNA:an R package for weighted correlation network analysis. BMC Bioinf. 2008;9:559.
[18] Shinozaki Y, Nicolas P, Fernandez-Pozo N, et al. High-resolution spatiotemporal transcriptome mapping of tomato fruit development and ripening. Nat Commun. 2018;9:364.
[19] Peng J, Wang H, Lu J, Hui W, Wang Y, Shang X. Identifying term relations cross different gene ontology categories. BMC Bioinf. 2017;18(Suppl 16):573.
[20] Sato N, Uematsu M, Fujimoto K, Uematsu S, Imoto IS. ggkegg: analysis and visualization of KEGG data utilizing the grammar of graphics. Bioinformatics. 2023;39:btad622.
[21] Yang L, Zhang YH, Huang F, Li Z, Huang T, Cai YD. Identification of protein-protein interaction associated functions based on gene ontology and KEGG pathway. Front Genet. 2022;13:1011659.

[22] Kanehisa M, Furumichi M, Sato Y, Kawashima M, Ishiguro-Watanabe M. KEGG for taxonomy-based analysis of pathways and genomes. Nucleic Acids Res. 2023;51:D587–92.
[23] Hillenmeyer S, Davis LK, Gamazon ER, Cook EH, Cox NJ, Altman RB. STAMS: STRING-assisted module search for genome wide association studies and application to autism. Bioinformatics. 2016;32:3815–22.
[24] Tran TD, Nguyen MT. C-Biomarker.net: a Cytoscape app for the identification of cancer biomarker genes from cores of large biomolecular networks. Biosystems. 2023;226:104887.
[25] Wei G, Sun L, Qin S, et al. Dme-Hsa Disease Database (DHDD): conserved human disease-related miRNA and their targeting genes in drosophila melanogaster. Int J Mol Sci. 2018;19:2642.
[26] Vlachos IS, Zagganas K, Paraskevopoulou MD, et al. DIANA-miRPath v3.0: deciphering microRNA function with experimental support. Nucleic Acids Res. 2015;43:W460–6.
[27] Xu W, Zhang Z, Yao L, et al. Exploration of shared gene signatures and molecular mechanisms between periodontitis and nonalcoholic fatty liver disease. Front Genet. 2022;13:939751.
[28] Justin GA, Girach A, Maldonado RS. Antisense oligonucleotide therapy for proline-23-histidine autosomal dominant retinitis pigmentosa. Curr Opin Ophthalmol. 2023;34:226–31.
[29] Tan R, Zhang G, Liu R, et al. Identification of early diagnostic and prognostic biomarkers via WGCNA in stomach adenocarcinoma. Front Oncol. 2021;11:636461.
[30] Scimone C, Granata F, Longo M, et al. Germline mutation enrichment in pathways controlling endothelial cell homeostasis in patients with brain arteriovenous malformation: implication for molecular diagnosis. Int J Mol Sci. 2020;21:4321.
[31] Kakularam KR, Canyelles-Nino M, Chen X, Lluch JM, Gonzalez-Lafont A, Kuhn H. Functional characterization of mouse and human Arachidonic Acid Lipoxygenase 15B (ALOX15B) orthologs and of their mutants exhibiting humanized and murinized reaction specificities. Int J Mol Sci. 2023;24:10046.
[32] Feugray G, Pereira T, Iacob M, et al. Determination of lipoxygenase, CYP450, and non-enzymatic metabolites of arachidonic acid in essential hypertension and type 2 diabetes. Metabolites. 2022;12:859.
[33] Xie T, Cai J, Yao Y, et al. LXA4 protects against blue-light induced retinal degeneration in human A2E-laden RPE cells and Balb-c mice. Ann Transl Med. 2021;9:1249.
[34] Xue Q, Kang R, Klionsky DJ, Tang D, Liu J, Chen X. Copper metabolism in cell death and autophagy. Autophagy. 2023;19:2175–95.
[35] Chrisnasari R, Hennebelle M, Vincken JP, van Berkel W, Ewing TA. Bacterial lipoxygenases: biochemical characteristics, molecular structure and potential applications. Biotechnol Adv. 2022;61:108046.
[36] Zhao T, Wang Y, Guo X, et al. Altered oxylipin levels in human vitreous indicate imbalance in pro-/anti-inflammatory homeostasis in proliferative diabetic retinopathy. Exp Eye Res. 2022;214:108799.
[37] Lin AL, Roman RJ, Regan KA, Bolch CA, Chen CJ, Iyer S. Eicosanoid profiles in the vitreous humor of patients with proliferative diabetic retinopathy. Int J Mol Sci. 2020;21:7451.
[38] Olivares-Gonzalez L, Salom D, Gonzalez-Garcia E, et al. NUTRARET: effect of 2-Year nutraceutical supplementation on redox status and visual function of patients with retinitis pigmentosa: a randomized, double-blind, placebo-controlled trial. Front Nutr. 2022;9:847910.
[39] Lee J-J, Chang-Chien G-P, Lin S, et al. 5-lipoxygenase inhibition protects retinal pigment epithelium from sodium iodate-induced ferroptosis and prevents retinal degeneration. Oxid Med Cell Longev. 2022;2022:1792894.
[40] Al-Shabrawey M, Mussell R, Kahook K, et al. Increased expression and activity of 12-lipoxygenase in oxygen-induced ischemic retinopathy and proliferative diabetic retinopathy: implications in retinal neovascularization. Diabetes. 2011;60:614–24.
[41] Scimone C, Donato L, Alafaci C, et al. High-throughput sequencing to detect novel likely gene-disrupting variants in pathogenesis of sporadic brain arteriovenous malformations. Front Genet. 2020;11:146.
[42] Elmasry K, Ibrahim AS, Saleh H, et al. Role of endoplasmic reticulum stress in 12/15-lipoxygenase-induced retinal microvascular dysfunction in a mouse model of diabetic retinopathy. Diabetologia. 2018;61:1220–32.
[43] Viita H, Kinnunen K, Eriksson E, et al. Intravitreal adenoviral 15-lipoxygenase-1 gene transfer prevents vascular endothelial growth factor A-induced neovascularization in rabbit eyes. Hum Gene Ther. 2009;20:1679–86.
[44] Lu Z, Zhang H, Zhang X, Gao Y, Yin ZQ. Lipoxin A4 delays the progression of retinal degeneration via the inhibition of microglial overactivation. Biochem Biophys Res Commun. 2019;516:900–6.
[45] Ahluwalia K, Du Z, Martinez-Camarillo JC, et al. Unveiling drivers of retinal degeneration in RCS rats: functional, morphological, and molecular insights. Int J Mol Sci. 2024;25:3749.
[46] Jeong HC, Shukla S, Fok WC, Huynh TN, Batista L, Parker R. USB1 is a miRNA deadenylase that regulates hematopoietic development. Science. 2023;379:901–07.
[47] Medina-Puche L, Lozano-Duran R. Plasma membrane-to-organelle communication in plant stress signaling. Curr Opin Plant Biol. 2022;69:102269.
[48] David R. Organelle dynamics: bridging the ER and plasma membrane. Nat Rev Mol Cell Biol. 2013;14:66–7.